Physical Modelling in Geotechnics
© 2022 KOREAN GEOTECHNICAL SOCIETY (KGS), Seoul, Korea, ISBN 978-89-952197-7-5

Dynamic model tests of levees reinforced by cement deep mixing method

H. Takahashi
Department of Geotechnical Engineering, PARI, MPAT, Japan

ABSTRACT: Levees made of soil can be damaged by the action of seismic forces, and liquefaction worsens the damage. In the past, huge tsunamis overcame coastal levees and tsunami overflow destroyed them. The author proposes the construction of a solidified soil wall in the levee using the cement deep mixing method and investigates its effectiveness and the design method. The application of the proposed method is expected to maintain the top height of the levee, even if the slope collapses because of earthquake motion and/or tsunami. The effects of seismic countermeasures, specifically the seismic characteristics of levees with an embedded grid-type improvement block at the centre, were investigated using centrifuge model tests. Consequently, the unimproved ground liquefied, and the slope of the levee collapsed owing to the vibration, while the top height of the levee was maintained. In addition, the strains on the surface of the improvement block were measured using strain gauges to investigate the stress state. Model tests were also conducted to examine the effects of different boundary conditions.

Keywords: earthquake, liquefaction, levee, cement deep mixing method, centrifuge.

1 INTRODUCTION

Coastal levees made of soil have been damaged by the action of seismic forces, with liquefaction worsening the damage. In the 2011 Great East Japan Earthquake, a huge tsunami overcame coastal levees after the earthquake and tsunami overflow destroyed them. In response to this, researchers (Nguyen et al., 2021; Takahashi, 2022) proposed the construction of a solidified soil wall in the levee using the cement deep mixing method (Kitazume and Terashi, 2013) and investigated its effectiveness and the design method. The construction of a solidified soil wall in the levee is expected to maintain the top height of the levee, even if the slope collapses because of earthquake motion and/or tsunami overflow (see Fig. 1).

The effects of seismic countermeasures are described in this paper. Specifically, the seismic characteristics of levees with an embedded grid-type improvement block at the centre were investigated by applying vibration in a centrifugal acceleration. In the model tests, the strains on the surface of the improvement block were measured using strain gauges to investigate the stress state. This information is important for considering the internal stability of the design method. Model tests were also conducted by varying the conditions at the bottom of the improvement block to examine the effects of different boundary conditions.

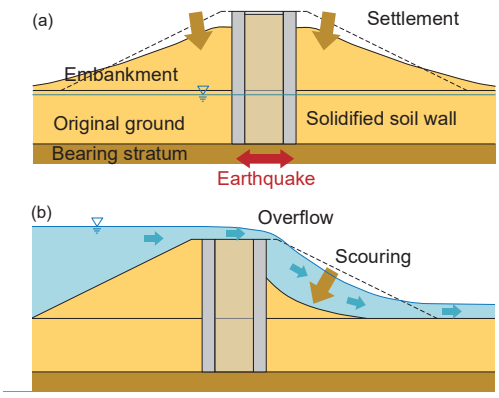

Fig. 1 Conceptual diagrams of proposed countermeasure

2 MODEL TEST CONDITIONS

Fig. 2 shows a schematic cross section of the model ground. The model was constructed as follows. First, a grease-coated membrane was attached to the wall to reduce the friction between the ground and the wall of the specimen container as much as possible. Accelerometers and pore water pressure gauges, which were buried in the ground, were hung from the wall with nylon ropes. Subsequently, Iide silica sand No. 7 (average grain size: 0.18 mm) was dropped in the air (see Takahashi et al., 2006) to form a bearing stratum with a relative density of approximately 90%. The improvement block was placed on the bearing stratum, and the original ground and embankment were made again using the air-fall method. Their relative density was approximately 50%, and they were liquefied underwater. The improvement block was manufactured by mixing Iide sand and a high early strength Portland cement slurry or using acrylic material to measure the strain. The improvement type is a grid-type (box-type) with improvement walls. Iide sand was also attached to the surface of the improvement block to generate a

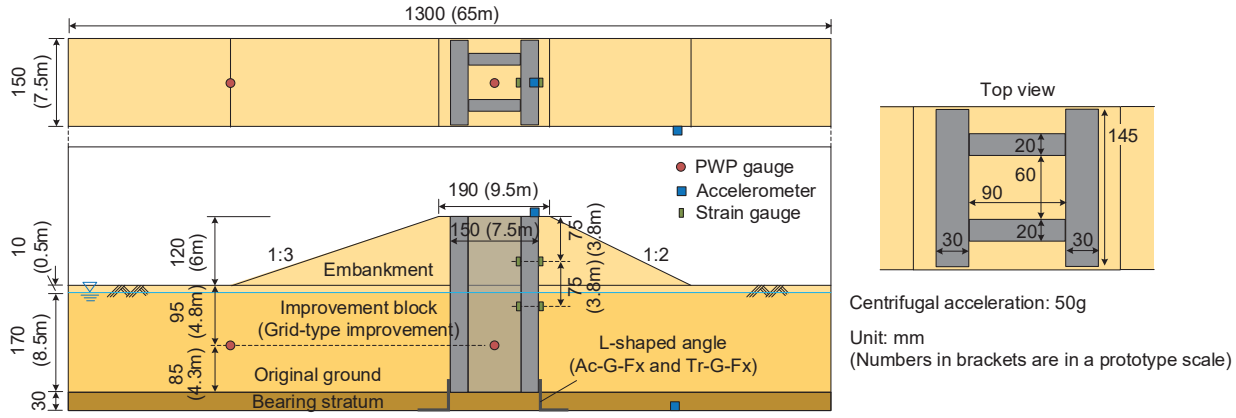

Fig. 2 Schematic cross section of model ground (Cases Ac-G, Tr-G, Ac-G-Fx, Tr-G-Fx)

Table 1. List of test cases

Name	Material	Improvement	Bottom condition
UN	–	–	–
Ac-G	Acryl	Grid type	Free
Tr-G	Solidified soil	Grid type	Free
Ac-G-Fx	Acryl	Grid type	Fixed
Tr-G-Fx	Solidified soil	Grid type	Fixed

frictional force against the ground.

The conditions of the five test cases are listed in Table 1, where one is the case without an embedded block and the others are the cases with embedded blocks. In the latter cases, the block material and fixed condition of the block bottom were varied. The vibration characteristics of these cases were investigated to determine the effects of the countermeasures. The unconfined compressive strength of the improved soil was approximately 1500 kN/m^2, comparable to that of the soil improved by the deep mixing method in the real field. Since it is difficult to attach strain gauges to the improved soil, an acrylic material to which strain gauges can be attached was used as the material for the improved soil in the strain measurement.

The ground model was set on a centrifuge platform and subjected to vibration tests under centrifugal force. The details of the centrifuge and shaking table used can be found elsewhere (Takahashi et al., 2019). Viscous fluid (kinematic viscosity: approximately 50 mm^2/s) was percolated into the ground from below using a water head difference, while the ground model was subjected to a centrifugal acceleration of 30*g*. After the water level was raised to the set height, the centrifugal acceleration was increased to 50*g*, and the ground model was vibrated.

In each test case, the vibrations were applied in three steps. Step 1 was a small vibration that did not cause any residual displacement in the ground. Steps 2 and 3 had the same large vibration. The input signal for all three vibrations was 50 sinusoidal waves of 50 Hz (1 Hz in a prototype scale). As an example, Fig. 3 shows the acceleration at the bottom of the container measured in Case UN (Step 2) in a prototype scale. It had a large acceleration of approximately 280 cm/s^2. In Steps 2 and 3, the ground liquefied, and a large deformation remained.

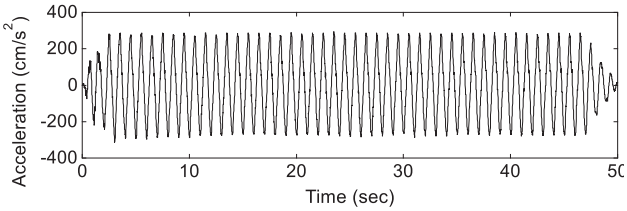

Fig. 3 Input acceleration to the model (Step 2 of Case UN)

3 TEST RESULTS

3.1 Ground deformation

Fig. 4 shows the models of Cases UN and Tr-G taken immediately after the vibration in Step 2. In Case UN, the original ground was displaced laterally, and the slope and toe of the embankment widened to the right and left. The top also sank significantly, which is similar to the liquefaction damage of embankments in general. However, in Case Tr-G, the slope and toe of the embankment widened, but the improvement block itself did not deform or fail. Therefore, the top height was maintained, and the effect of the countermeasures was evident. Although the displacement of the slope and toe was larger than that of the existing countermeasure method, the characteristic of this method that the top height of the improvement block is maintained was clearly shown. The settlement of the sandy soil between the grid walls was caused by the sand falling into the gap between the grid wall and the glass window of the specimen container, and the settlement of the sandy soil inside the grids was small. After the three steps of vibration, the settlement of the embankment top was measured in the gravity field, and it reached 294 cm in the prototype scale in Case UN, while it was only 25 cm at the top of the grid wall and 43 cm at the ground surface

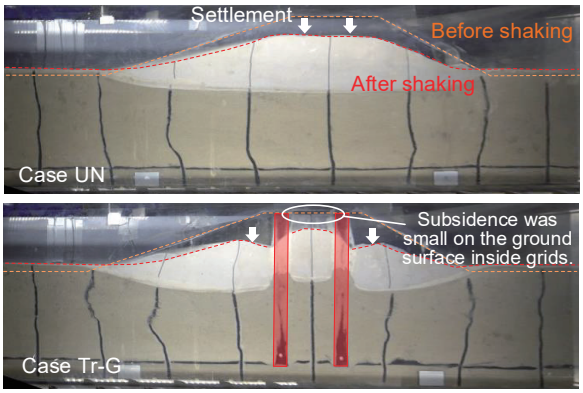

Fig. 4 Model ground after vibration of Step 2

inside the grids in Case Tr-G. The difference in the settlements at the top of the grid wall and the ground inside the grids was small, and it was found that this countermeasure was effective from the viewpoint of the use of the embankment top after an earthquake.

3.2 Excess pore water pressure

Fig. 5 shows the time histories of excess pore water pressure measured in the lower part of the embankment toe and at the ground under the embankment or inside the grids (G.L. −4.75 m) in Step 2. The time was in a prototype scale. The figure also indicates the effective overburden pressure as a dashed line. In all cases, the excess pore water pressure reached the effective overburden pressure under the toe 3 s after the start of vibration, and it was maintained at more than 100 s after the vibration. This indicates that the ground was sufficiently liquefied.

In Case UN, the excess pore water pressure in the lower part of the embankment did not reach the effective overburden pressure. This may be because the groundwater table was lowered by the settlement of the embankment, pore water pressure itself was lowered, and effective overburden pressure was also lowered by the expansion of the embankment. Although the pore water pressure did not appear to have increased, the original ground was deformed significantly during the vibration, and it is believed that the original ground was also liquefied under the embankment.

In Case Ac-G, the pore water pressure was measured inside the grids; it was not affected by the lowering of the groundwater table or the spreading of the embankment. As the figure shows, it did not increase up to the effective overburden pressure and did not lead to liquefaction. However, in Case Tr-G, the excess pore water pressure reached the effective overburden pressure. As described later, the vibration of the improvement block, in this case, was too large to prevent liquefaction. However, the pore pressure decreased immediately after the vibration, and the degree of liquefaction was low. It has been found that the degree of liquefaction inside the grids is smaller (e.g., Takahashi et al., 2006). In addition,

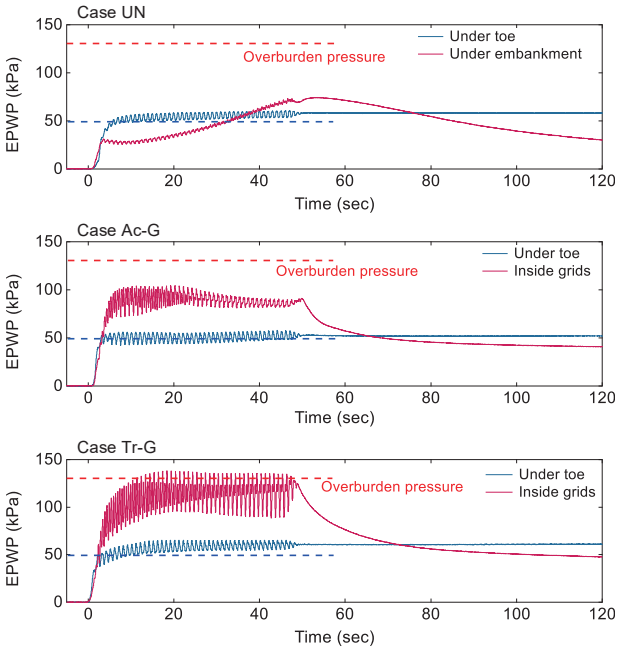

Fig. 5 Time histories of excess pore water pressure (Step 2)

the settlement of the ground surface inside the grids is small, even when the pore water pressure increases. If the force resulting from the increasing pore water pressure is considered in the strength design of the improved soil, grid-type improvement can be used as a countermeasure without the need for full embankment improvement.

3.3 Acceleration characteristics

Fig. 6 shows the response acceleration measured at the embankment top in Case UN and at the top of the improvement block in the other cases. In Case UN, the acceleration after the fourth wave was smaller than that shown in Fig. 3, indicating that the liquefied ground became a seismic isolation layer and the vibration was not transmitted to the top. In addition, the acceleration remained because of the repeated vibration, and the direction of the accelerometer changed from the horizontal direction owing to the loosening of the ground.

In Cases Ac-G and Tr-G, the acceleration was reduced after the fourth wave, and the vibration was not amplified. Comparing the reduction rates of Ac-G and Tr-G, the ratio of Ac-G was larger than that of Tr-G. This may result from the higher inertia of the improvement block in Case Tr-G, which has a higher mass than the acrylic material. The reason why the acceleration of the improvement block was smaller than the input acceleration is considered the sliding on the bottom of the improvement block. In the design of the deep mixing method, sliding is generally not allowed to avoid residual displacement of the improvement block. For this reason, in Cases Ac-G-Fx and Tr-G-Fx, it was assumed that there was no sliding. In these cases, L-shaped angles were used to prevent the bottom of the improvement

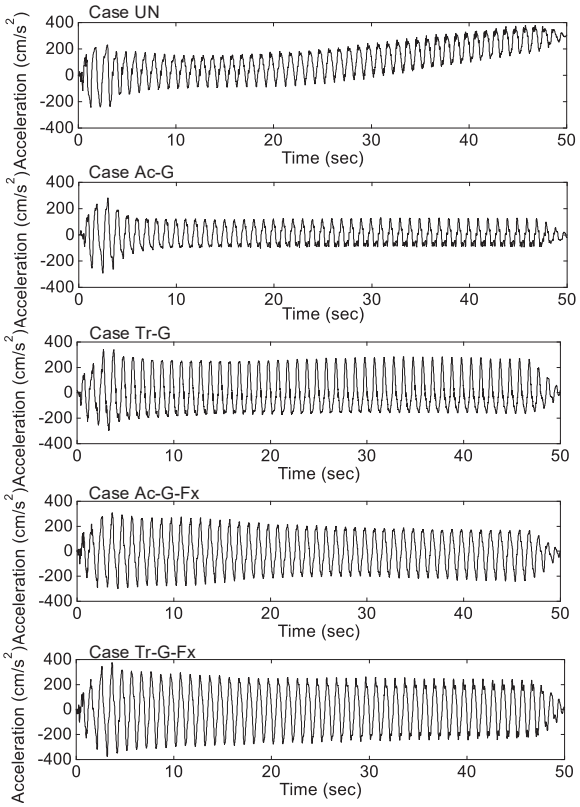

Fig. 6 Time histories of acceleration (Step 2)

block from sliding. The acceleration at the top was amplified slightly against the input acceleration. Considering the increased acceleration, it is possible to design an improvement block to allow sliding.

3.4 Stress state of solidified soil walls

In Cases Ac-G and Ac-G-Fx, strain gauges were attached to the acrylic improvements to measure the strain. The compressive and tensile stresses at the surface of the improvement block were calculated from the strains. The time histories are shown in Fig. 7. The compressive and tensile stresses were positive and negative, respectively. The vertical tensile stresses generated were small because of the grid-type improvement. Horizontal bending failure of the wall is a problem in the case of grid-type improvement. As shown in the figure, tensile stress was generated in the inner wall of the grid, suggesting that the wall was bent by the earth pressure from outside the grid. However, the value of the tensile stress was less than approximately 150 kN/m^2, which was not significant. In fact, no damage, such as bending failure, was observed after the tests in Cases Tr-G and Tr-G-Fx.

4 CONCLUSIONS

The seismic characteristics of levees with an embedded grid-type improvement block at the centre were investigated using vibration tests in a centrifugal acceleration. It was confirmed that the slope of the embankment collapsed, but the top height of the improvement block was maintained under earthquake motion. This method can also be applied to river levees, which are also damaged by earthquakes and/or overflow.

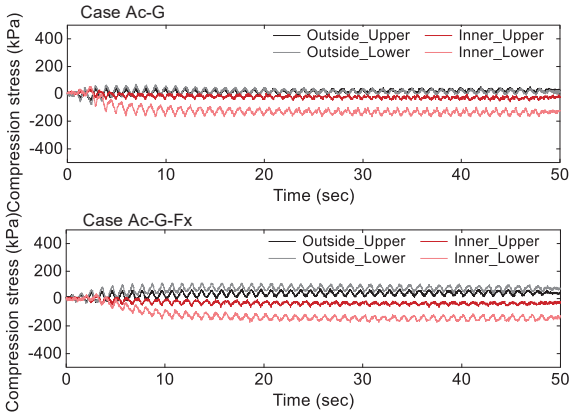

Fig. 7 Horizontal compressive and tensile stresses (Step 2)

ACKNOWLEDGEMENTS

This study was supported by the Port and Harbor Bureau of the Ministry of Land, Infrastructure, Transport and Tourism (MLIT) of Japan, and the author would like to express gratitude to the members of the CDM association for providing information and to Mr. Satoshi Saito of Geodesign Co. for his cooperation in the tests.

REFERENCES

Kitazume, M. and Terashi, M. 2013. *The deep mixing method*. CRC press.

Nguyen, B., Ueno, K., Morikawa, Y., Takahashi, H. and Tokunaga, S. 2021. Study on the earthquake resistance of deep-mixing reinforced levee using effective stress analysis. *Proc. of Deep Mixing Conference 2021*: 820-829.

Takahashi, H. 2022. Tsunami overflow tests of levee reinforced by deep mixing method in centrifuge. *Proc. of the 20th International Conference on Soil Mechanics and Geotechnical Engineering (ICSMGE)*. (in press)

Takahashi, H., Fujii, N., Morikawa, Y. and Takano, D. 2019. Development of hydro-geotechnical centrifuge PARI Mark II-R. *Technical Note of the Port and Airport Research Institute*, No. 1353: 27p.

Takahashi, H., Kitazume, M. and Ishibashi, S. 2006. Effect of deep mixing wall spacing on liquefaction mitigation. *Proc. of the 6th International Conference on Physical Modelling in Geotechnics*: 585-590.

Takahashi, H., Kitazume, M., Ishibashi, S. and Yamawaki, S. 2006. Evaluating the saturation of model ground by P-wave velocity and modelling of models for a liquefaction study. *International Journal of Physical Modelling in Geotechnics* 6 (1): 13-25.